Water Air Soil Pollut (2016) 227: 337
DOI 10.1007/s11270-016-3032-7

Mesoporous Magnetic Ferrum-Yttrium Binary Oxide: a Novel Adsorbent for Efficient Arsenic Removal from Aqueous Solution

Chao Qin · Liping Liu · Yijie Han · Cheng Chen · Yeqing Lan

Received: 12 February 2016 / Accepted: 3 August 2016 / Published online: 20 August 2016

Abstract Mesoporous magnetic ferrum-yttrium (Fe-Y) binary oxide was first synthesized as an effective absorbent for the removal of arsenite [As(III)] and arsenate [As(V)] from aqueous solution. The adsorbent was characterized by field emission scanning electron microscopy (FESEM), energy dispersion X-ray spectrometer (EDX), vibrating sample magnetometer (VSM), X-ray photoelectron spectra (XPS). A series of batch experiments were conducted to estimate the adsorption capacity of arsenic and to investigate the effect of solution pH and coexisting anions on the removal of arsenic. The results demonstrate that the adsorption of arsenic by the adsorbent was pH-dependent. The optimal adsorption was realized at pH 4 for As(V) and at pH 5 for As(III). The maximum capacity of As(V) and As(III) obtained in this study was 200 and 73 mg g^{-1}, respectively. The anions concluding sulfate, chloride, and nitrate exerted a weak impact on As(V) removal, whereas phosphate greatly suppressed the adsorption of both As(III) and As(V) through competing with arsenic species for active adsorption sites on the surface of the adsorbent. All above suggest that the novel adsorbent not only works efficiently for arsenic removal, but also is stable in a wide solution pH range, which is conducive to the practical application for wastewater treatment.

Keywords Ferrum-yttrium binary oxide · Magnetic · Mesoporous · Arsenic · Adsorption

1 Introduction

Due to natural sources and anthropogenic activities, arsenic (As) contamination in natural surface water and ground water has been frequently reported through the world, which has led to a serious health threat to the human beings. It has been pointed that long-term exposure to water contaminated by arsenic even at a very low concentration level could cause the cancers of the skin, lung, liver, kidney etc., (Karim 2000). Therefore, the maximum contaminant level of arsenic in drinking water was reduced from 50 to 10 μg L^{-1} by the US Environmental Protection Agency in 2006 (Vrijenhoek and Waypa 2000). Arsenic carcinogenicity and the stricter standard on arsenic concentration in drinking water have stimulated great efforts to develop economic and efficient approaches for arsenic removal from aqueous solution.

In natural environments, arsenic exists mainly in two oxidation states, As(III) and As(V). As compared with As(V), As(III) is more toxic and mobile (Jiang et al. 2015). Consequently, the conversion of As(III) to As(V) by oxidants followed by precipitation or adsorption is usually considered to be a feasible method to minimize arsenic contamination (Zhang et al. 2007; Bordoloi et al.

Electronic supplementary material The online version of this article (doi:10.1007/s11270-016-3032-7) contains supplementary material, which is available to authorized users.

C. Qin · L. Liu · Y. Han · C. Chen · Y. Lan (✉)
College of Sciences, Nanjing Agricultural University, Nanjing 210095, China
e-mail: lanyq102@njau.edu.cn

2013; Jiang et al. 2015; Bai et al. 2016; Kyzas et al. 2016; Zhang et al. 2016). The common treatment approaches for removing arsenic from aqueous solution are still involved in coagulation-flocculation (Lee and Rosehart 1972; Li et al. 2006; Mondal et al. 2013), adsorption (Reddy et al. 2013; Zhang et al. 2013; Asadullah et al. 2014; Ungureanu et al. 2015), membrane technology (Mondal et al. 2014; Zhao et al. 2016), and ion exchange (Bellack 1971). Among these approaches mentioned above, adsorption for arsenic removal attracts much more attention and has been widely utilized owing to its high efficiency, easy operation, and low cost.

It has been reported that the combination of some rare metal salts together with relatively abundant heavy metal salts or their compounds can further enhance the adsorption capacities for arsenic uptake in aqueous systems (Zhang et al. 2005; Ren et al. 2011; Yu and Chen 2014). For instance, Yu et al. (2015) reported that an yttrium-manganese binary composite displayed extremely high adsorption capacity for arsenate removal and the maximum adsorption capacity of 279.9 mg g^{-1} was achieved at pH 7, much higher than most reported adsorbents up to now. Wasay et al. (1996) discovered that a basic yttrium carbonate was able to effectively remove arsenite and arsenate, and the maximum adsorption capacity for both anions was up to 400 mg g^{-1} or more under the optimal pH conditions. Nevertheless, these adsorbents still expose some drawbacks in the field of practical application in treating arsenic-contaminated water. For example, it is usually difficult to separate the adsorbents with micron to nanometer particles from water after adsorbing arsenic. In addition, the industrial effluent containing arsenic is typically acidic. It was observed that the pH in arsenic-containing wastewater from a sulfuric acid factory was 2 (Wang et al. 2011). Under such an acidic condition, basic yttrium carbonate as an adsorbent can be severely dissolved, which limits its applications although it exhibits extremely high adsorption capacity for arsenic. It has been also found that a relatively severe dissolution of yttrium-manganese binary composite as an adsorbent for arsenic removal occurred at pH 3 or lower (Yu et al. 2015). Therefore, it is very meaningful and necessary to develop a new type of adsorbent that not only works efficiently for arsenic removal due to excellent adsorption ability and strong magnetic, but also is stable in a wide solution pH range.

In this study, a novel mesoporous magnetic ferrum-yttrium (Fe-Y) binary oxide was first synthesized. The structural characteristics of the adsorbent were studied by field emission scanning electron microscopy (FESEM) with energy dispersive X-ray (EDX), X-ray photoelectron spectroscopy (XPS), the analysis of pore size distribution, and the determination of point zero charge. A series of batch adsorption experiments were conducted to further investigate the adsorption capacity, the adsorption kinetics and isotherms, as well as the impacts of solution pH and coexisting anions on arsenic removal.

2 Materials and Methods

2.1 Reagents

The chemicals including $Y(NO_3)_3 \cdot 6H_2O$, $FeSO_4 \cdot 7H_2O$, Na_2SO_4, NaCl, NaOH, HNO_3, $NaNO_3$ and $Na_2HPO_4 \cdot 12H_2O$ were of reagent grade and provided by Xilong Chemical Co., Ltd. (China). As_2O_3 and $Na_2HAsO_4 \cdot 7H_2O$ also were of reagent grade and purchased from Sigma-Aldrich. The stock solutions of As(III) and As(V) were prepared by dissolving As_2O_3 in diluted NaOH solution and dissolving $Na_2HAsO_4 \cdot 7H_2O$ in deionized water, respectively. The standard solution (1000 mg L^{-1}) for arsenic analysis was purchased from the National Institute of Metrology of China and was diluted with deionized water from STILL ACE SA-2100E1 Water-system (Tokyo Rikakikai, Japan) to the desired concentrations.

2.2 Preparation of Fe-Y Binary Oxide

Fe-Y binary oxide was prepared through an ultrasonic co-oxidation precipitation method. Briefly, 3.83 g $Y(NO_3)_3 \cdot 6H_2O$ and 8.34 g $FeSO_4 \cdot 7H_2O$ were first dissolved in 100 mL deionized water at room temperature. The mixed solution was continuously bubbled with oxygen for 5 min, and then 5 M NaOH solution was added dropwise to the mixed solution under ultrasonic condition. When the color of the formed precipitate changed from ink green to black, the mixed solution was stopped bubbling with oxygen but still kept ultrasonic for 20 min. The obtained precipitate was separated from the solution

with a strong magnet, and then the collected precipitate was washed with deionized water and absolute ethyl alcohol for three times, respectively. Finally, the particles were dried at 60 °C for 6 h and the pulverized dry material was stored in a desiccator prior to use.

2.3 Characterization of Fe-Y Binary Oxide

2.3.1 Field Emission Scanning Electron Microscopy

The adsorbent sample was first coated with a thin film of platinum for electric conductivity. A field emission scanning electron microscope (Hitachi S-4800, Japan) equipped with an energy dispersion X-ray spectrometer with the working distance of 2.5 μm and an accelerating voltage of 20.0 kV was used to observe the surface morphology and chemical constituents of Fe-Y binary oxide.

2.3.2 Specific Surface Area

The specific surface area of the adsorbent was measured using the Brunauer-Emmett-Teller (BET) gas adsorption isotherm with N_2 on a surface area and porosimetry analyzer (V-sorb 2800P, China). Before the measurement, the sample was degassed with N_2 for 2 h at 120 °C in a vacuum line. And the pore size distributions were derived from the desorption branches of the isotherms using the Barrett-Joyner-Halenda (BJH) model.

2.3.3 Magnetic Hysteresis Loop

Magnetic property of the adsorbent was measured using a vibrating sample magnetometer (VSM) (EV7, USA) at room temperature.

2.3.4 Point of Zero Charge

The point of zero charge (pH_{pzc}) of the adsorbent is an important parameter to estimate the adsorption property at different solution pH, and it was determined according to the method described by Zhang et al. (2013) and Yu et al. (2015). Briefly, Fe-Y binary oxide was first suspended in 0.01 M $NaNO_3$ for 24 h. And then, a 50 mL suspension was adjusted to the desired pH values ranging from 4 to 10 with a diluted NaOH or HNO_3 solution. After equilibrium, the initial pH (pH_i) was measured. Then, 1.5 g $NaNO_3$ was introduced into each suspension. After shaking for 24 h, the final pH (pH_f) was determined. The pH_{pzc}, as the pH at which ΔpH equals 0, was obtained by plotting ΔpH ($pH_f - pH_i$) against pH_f.

2.3.5 X-ray Photoelectron Spectroscopy

X-ray photoelectron spectra were collected on an ESCALAB 250Xi (Thermo Scientific) with a monochromatic Al Ka X-ray source (1486.6 eV). C1s peaks were used as an inner standard calibration peak at 284.7 eV. For wide scan spectra, an energy range of 0–1100 eV was used with pass energy of 80 eV and step size of 1 eV. The high-resolution scans were conducted according to the peak examined with pass energy of 40 eV and step size of 0.05 eV. The XPS results were collected in binding energy forms and fitted using a nonlinear least-square curve fitting program (XPSPEAK41Software).

2.3.6 Batch Adsorption Experiments

Batch adsorption experiments were performed to investigate the impacts of various parameters on the adsorption efficiency of As(III) and As(V) by Fe-Y binary oxide. To determine the adsorption capacity at an initial pH 5, the adsorbent (10 mg) was added to 50 mL solution with 10, 20, 30, 40, 50, 60, 70, 80, 90, and 100 mg L^{-1} As(III) or As(V), respectively, and the mixed solution was vigorously agitated in a shaker at 180 rpm to reach equilibrium. At desired time intervals, aliquot 1 mL of the mixed solution was sampled. Then, the suspension was filtered through a 0.22-μm polyethersulfone membrane. The filtrate was analyzed for residual arsenic concentration. All batch experiments were conducted at 25 °C. In order to investigate the effect of pH on the arsenic adsorption, batch experiments were conducted at the initial solution pH ranging from 3 to 12, which was adjusted with diluted NaOH or HNO_3 solution. The final pH of the solution was also determined by the end of the batch adsorption experiments. It should be pointed that in this study, the solution pH did not maintain with buffers to minimize the competition of other anions with As(III) or As(V) for active adsorption sites on the surface of the adsorbent. To further investigate the influence of coexisting anions including sulfate, chloride, nitrate, and phosphate on the adsorption of arsenic by the adsorbent, the corresponding

sodium salts with 10 times of the initial arsenic concentration were introduced into the reaction system. All the batch adsorption experiments in the section were performed in triplicate, and the average values were reported, together with error bars represented.

2.4 Analytic Methods

The concentrations of As(III) and As(V) before and after adsorption were analyzed by an inductively coupled plasma optical emission spectrometer (ICP-OES, PerkinElmer Optima 3000). Sartorius PB-10 acidity meter (Beijing) was used to measure the pH values for different reaction solutions after three-point calibration.

The concentration of Y was determined by a colorimetric method using aluminon as a chromogenic agent. The solution pH was adjusted using diluted NaOH and HCl for the color development. The absorbance was measured in a 1-cm cell at 528 nm on an Alpha-1502 UV–VIS spectrometer (Shanghai Puyuan, China). The liner range of this method was 2 to 9 mg L^{-1}. The recovery range and relative standard deviation (RSD) were 99.05 to 101.76 and 0.15 %, respectively.

3 Results and Discussion

3.1 Characterization of Fe-Y Binary Oxide

The morphology of the synthesized Fe-Y binary oxide examined by FESEM is illustrated in Fig. 1a, which demonstrates that the obtained adsorbent is aggregated by nanograins (around 40 nm). This highly scattered adsorbent is very beneficial to the transportation of arsenic onto its surface. Based on the analysis of EDX presented in Fig. 1b, it is concluded that the adsorbent is mainly consisted of two metal elements including Fe and Y and the molar ratio of Fe to Y is approximately 2:1. The analysis of BET indicates that the binary oxide has a specific surface area of 99.43 $m^2\ g^{-1}$ with a pore volume of 0.4197 $cm^3\ g^{-1}$. The pore size distribution of the binary oxide is illustrated in Fig. 1c, which suggests that Fe-Y binary oxide obtained in this study is a mesoporous material.

The pH_{pzc} of the adsorbent was determined, and its value was approximately 7.17 obtained from Fig. 1d. This implies that the surface of the adsorbent is positively charged at the solution pH < 7.17, and it becomes negatively charged at the solution pH > 7.17.

The magnetic property of Fe-Y binary oxide was characterized by VSM at room temperature, and its magnetic hysteresis loop is illustrated in Fig. 2. The values of saturation magnetization (Ms), coercivity (Hc), and squareness (Sr = remnant magnetization (Mr)/(Ms)) for the adsorbent were determined to be 34.14 emu g^{-1}, 7.60 Oe, and 0.203, respectively. These values were smaller than those of the theoretical specific saturation magnetization of bulk magnetite (Zaitsev et al. 1999) due to the effect of small particle surface of the adsorbent and the introduction of yttrium. An adsorbent with strong magnetic is very conducive to improve the efficiency of separation between adsorbent and wastewater. The inset in Fig. 2 exhibits that the mixed solution was highly dispersed before an external magnetic field was applied, meaning that the separation is difficult. However, the adsorbent particles were strongly attracted to the wall of bottle by a magnetic field in a very short time (a few seconds) and the mixed solution rapidly became clear. This demonstrates that the adsorbent can be easily and quickly separated from water.

3.2 Adsorption Kinetics

Figure 3 shows the variation of the adsorption capacities of As(V) and As(III) on Fe-Y binary oxide with the reaction time at the initial pH 5 and initial arsenic concentration = 80 mg L^{-1}. It is noted from Fig. 3 that the adsorption capacities of As(V) and As(III) on Fe-Y binary oxide were significantly improved as compared with those of control (Fe_3O_4, data not presented in Fig. 3), especially for As(V). For instance, the adsorption capacity of As(V) by Fe-Y binary oxide at 10-h equilibrium reached to 180 mg g^{-1}, approximately seven times as high as that of control. The adsorption capacity of As(III) also increased from 56 mg g^{-1} on the surface of Fe_3O_4 to 71.4 mg g^{-1} on the surface of Fe-Y binary oxide within 18-h equilibrium. These results confirm that an introduction of yittrium can greatly enhance the removal efficiency of arsenic. By observing the whole adsorption process, it is still found that the adsorption rate of As(III) by Fe-Y binary oxide was much slower than that of As(V). Similar results were reported by Martinson and Reddy (2009) and Zhang et al. (2013) during investigating the adsorption of

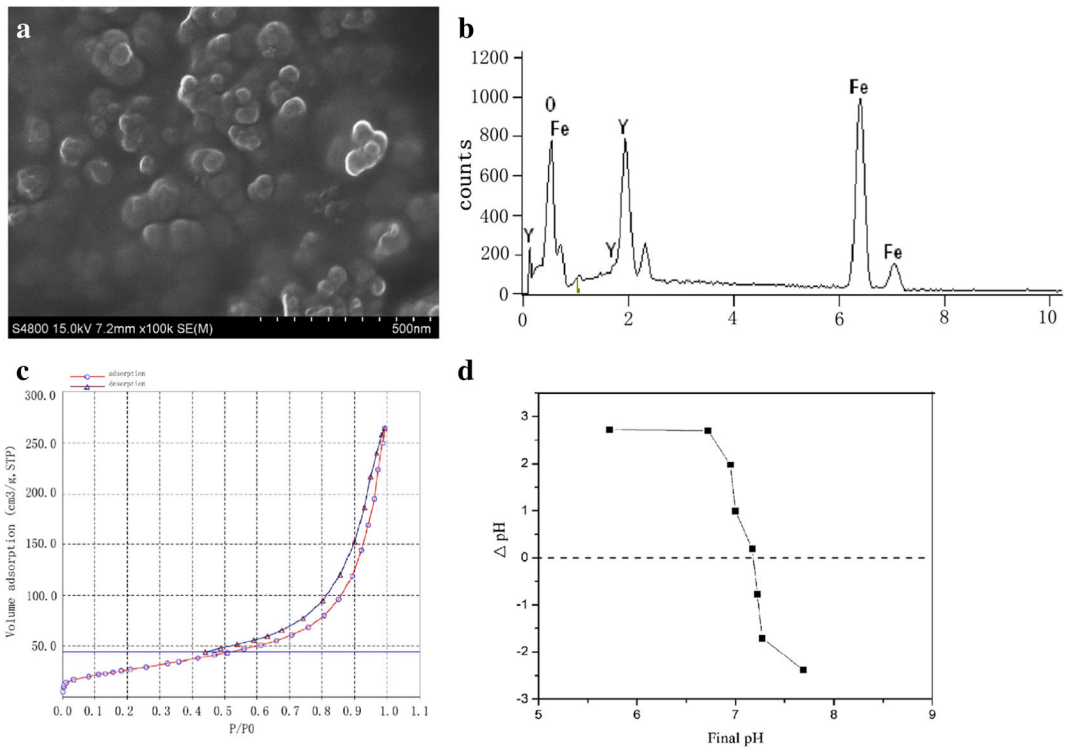

Fig. 1 Characterization of Fe-Y binary oxide: **a** FESEM image, **b** EDX image, **c** pore size distribution, and **d** point of zero charge

As(V) or As(III) by pure cupric oxide and Fe-Cu binary oxide.

Yu et al. (2015) reported that the experimental data for As(V) removal by Y-Mn binary composite can be better described by the pseudo-second-order model with a higher value of correlation coefficient than by the pseudo-first-order model. Thus, in this study, the pseudo-second-order model was adopted to further discuss the adsorption process. The pseudo-second-order model is generally expressed as

$$\frac{t}{q_t} = \frac{1}{kq_e^2} + \frac{1}{q_e} \tag{1}$$

where q_e and q_t represent the adsorption capacities

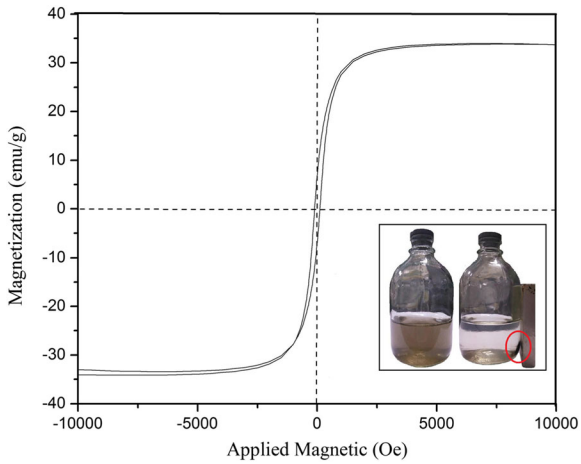

Fig. 2 Magnetic hysteresis loop and photograph of the separation process of magnetic microspheres

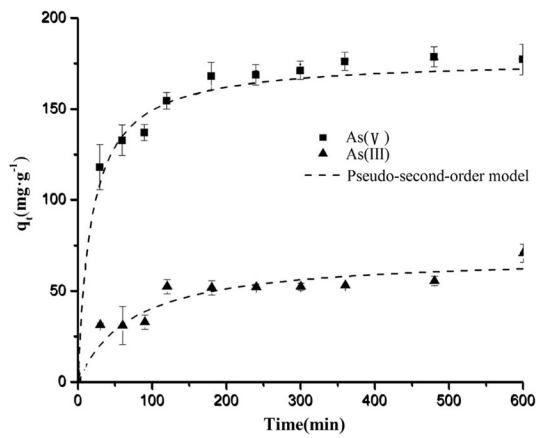

Fig. 3 The fitted results of adsorption kinetic models. Arsenic initial concentrations = 80 mg L^{-1}, adsorbent dose = 200 mg L^{-1}, and temperature = 25 °C

(mg g^{-1}) of As on Fe-Y binary oxide at equilibrium and at time t (min), respectively; k (mg g^{-1} min^{-1}) is the related adsorption rate constant. The kinetic model well fit the data over the entire course of the experiment (Fig. 3). Model parameters including correlation coefficients, maximum uptake capacities, and the kinetic constants are listed in Table 1. The theoretical q_e values predicted by Eq. (1) are very close to the experimental q_e values obtained in this study (see Table 1). Therefore, it is concluded that the kinetics of arsenic adsorption on the surface of Fe-Y binary oxide can be also described by pseudo-second-order kinetics model. In addition, this suggests that the adsorption process might be chemical adsorption. The plausible mechanism of arsenic adsorption could be proposed as below:

$$M{-}OH(s) + H_3AsO_3(H_3AsO_4) \rightleftharpoons M^{+}\text{-}H_3AsO_3(H_3AsO_4)(s) + OH^{-} \quad (2)$$

$$M{-}OH(s) + H_2AsO_3^{-}(H_2AsO_4^{-}) \rightleftharpoons M\text{-}H_2AsO_3(H_2AsO_4)(s) + OH^{-} \quad (3)$$

Where (s) stands for the solid phase. The suggested mechanism is well in agreement with the observed pH increase in the equilibrium solution.

3.3 Adsorption Isotherms

The adsorption capacities of As(III) and As(V) on Fe-Y binary oxide were further investigated by adsorption isotherms. Figure 4 shows the adsorption amounts of As(III) and As(V) increased with the initial concentrations of arsenic from 10 to 100 mg L^{-1} at pH = 5 and 25 °C. In this section, to evaluate the saturated adsorption capacity of the adsorbent and calculate various adsorption parameters, two commonly used isotherm models (Langmuir and Freundlich) are employed.

$$\text{Langmuir}: qe = KLQmCe/(1 + KLCe) \quad (4)$$

$$\text{Freundlich}: qe = KFCe^{1/n} \quad (5)$$

Table 1 The pseudo-second-order kinetic parameters of As(III) and As(V) adsorption

Metal	The pseudo-second-order		
Ion	q_e(mg g^{-1})	k (g mg^{-1} min^{-1})	R^2
As(V)	174 (180*)	3.17×10^{-4}	0.9985
As(III)	62 (71.4*)	2.63×10^{-4}	0.9555

* The experimental q_e values

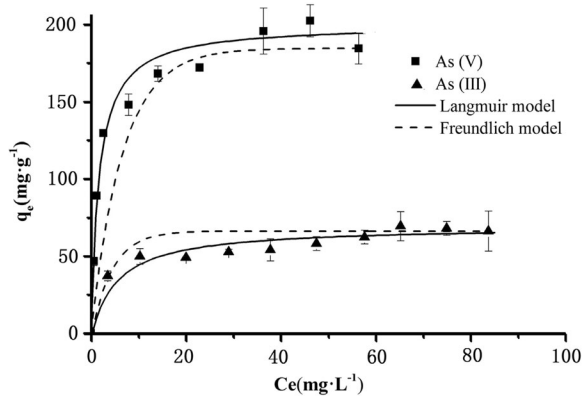

Fig. 4 Adsorption isotherms of As(V) and As(III) by Fe-Y binary oxide fitted by Langmuir model and Freundlich model, respectively. Adsorbent dose = 200 mg L^{-1}, pH = 5, and temperature = 25 °C

Where q_e and C_e represent the adsorption capacity (mg g^{-1}) and the concentration (mg L^{-1}) of arsenic at equilibrium, respectively. Q_m (mg g^{-1}) and K_L stand for the saturated adsorption capacity and the equilibrium adsorption constant, respectively; K_F and n are Freundlich constants corresponding to adsorption capacity and adsorption intensity, respectively.

The simulated isotherms are plotted in Fig. 4. The calculated isotherm parameters are listed in Table 2. By comparison of the regression coefficients (R^2) of the two models, it is noted that the adsorption behavior of arsenic on Fe-Y binary oxide can be better described by Langmuir model than the Freundlich model. It is also found that As(V) is more fitted to Langmuir model than As(III) did. These results suggest that the surface of Fe-Y binary oxide is relatively homogeneous, and the adsorption for arsenic occurs mainly as monolayer. Besides, the calculated maximum adsorption capacity of Fe-Y binary oxide was 200 mg g^{-1} for As(V) and 73 mg g^{-1} for As(III), which are close to those obtained in Section 3.2 (see Table 1). To estimate the performance of Fe-Y binary oxide for arsenic removal, the Q_m value was compared with the results from literature (Zhang et al. 2007, 2012, 2013; Ren et al. 2011; Yu et al. 2015) for different adsorbents (see Table 3). Though it is hard to make direct comparison since the adsorption capacities of different adsorbents for arsenic were obtained under different conditions, it is concluded that the mesoporous magnetic Fe-Y binary oxide was quite efficient for both As(V) and As(III) removal from aquatic solution.

Table 2 Parameters of the Langmuir and Freundlich isotherms of arsenic adsorption by Fe-Y binary oxide

Metal	Langmuir model			Freundlich model		
Ion	R^2	Qm (mg g^{-1})	K_L(L mg^{-1})	R^2	n	K_F (L mg^{-1})
As(V)	0.9944	200	0.5051	0.8431	3.774	76.03
As(III)	0.9833	73	0.1330	0.9185	5.621	30.65

3.4 Effect of pH

In our preliminary study, it was observed that the concentrations of Fe and Y were very low and almost could not be detected in the pH range of 3 to 12 although the adsorbent was continuously stirred for 24 h at 25 °C, which suggests that in such a wide pH range Fe-Y binary oxide is very stable. Nevertheless, the concentrations of Fe and Y increased obviously when the solution pH was 2, meaning that the dissolution of Fe-Y binary oxide occurs at pH ≤ 2. Therefore, in this study, the effect of pH on the adsorption of arsenic by Fe-Y binary oxide was investigated in the pH range of 3 to 12 and the results are illustrated in Fig. 5. It is noted that the removal efficiency of arsenic by the adsorbent is obviously dependent on the solution pH. The adsorption of As(V) is more effective than that of As(III) in a pH range from 3 to 10. However, As(III) is more effectively removed than As(V) at pH > 10. The optimal adsorption of As(V) was realized at pH 4, and in the case, the initial As(V) in the solution was almost completely removed. The adsorption behavior of As(III) is different from that of As(V), the optimal adsorption of As(III) was achieved at pH 5.

Generally, the adsorption of As(V) by solid adsorbent is more dependent on pH than that of As(III) (Zhang et al. 2013). The effect of pH on the adsorption of As(V) by Fe-Y binary oxide is very similar to the results reported by Ren et al. (2011), which is related with the arsenate species in aquatic solution and the pH_{pzc} of Fe-Y binary oxide. The dominant species of As(V) are $H_2AsO_4^-$ and $HAsO_4^{2-}$ in the pH range of 3 to 10 (Yu et al. 2015). On the other hand, as described previously that the pH_{pzc} of Fe-Y binary oxide was 7.17, this means that As(V) is favorably attracted to the surface of Fe-Y binary oxide at a low pH range (<7.17) due to electrostatic attraction, contributing to a high As(V) removal efficiency. Nevertheless, it is noted that the removal of As(V) is relatively not efficient at pH 3, which is possibly attributed to arsenate species (H_3AsO_4 exists as one of the dominant species of arsenate (Yu et al. 2015)). On the contrary, the surface of Fe-Y binary oxide will be carried with negative charges at pH > 8, leading to a decrease in the adsorption of As(V) with pH increasing owing to the electrostatic repulsion. The arsenite species are H_3AsO_3, $H_2AsO_3^-$, and $HAsO_3^{2-}$ in the pH range of <8, 8–11, and >12, respectively (Wasay et al. 1996). Consequently, the adsorption of As(III) by the adsorbent is obviously weaker than that of As(V) at pH < 8. Since the charges carried by the species of As(III) and As(V) are similar at pH > 11, almost the same removal efficiency of arsenic is obtained.

Table 3 Comparison of maximum arsenic adsorption of different binary oxide adsorbents

Adsorbent	Arsenic conc. (mg L^{-1})	Max. adsorption of As(V) (mg g^{-1})	Max. adsorption of As(III) (mg g^{-1})	Ref.
Fe-Cu binary oxide	0–60	82.7	122.3	Zhang et al. 2013
Fe-Mn binary oxide	0–40	53.9	100.4	Zhang et al. 2007
Fe-Zr binary oxide	0–40	46.1	120.0	Ren et al. 2011
Y-Mn binary composite	0–100	279.9	28.0	Yu et al. 2015
Zr-Mn binary hydrous oxide	0–25	80	104	Zhang et al. 2012
Fe-Y binary oxide	0–100	200	73	This study

3.5 Influence of Coexisting Anions

The effect of coexisting anions including sulfate, chloride, nitrate, and phosphate on arsenic adsorption by Fe-Y binary oxide at pH 5 was investigated, and the results

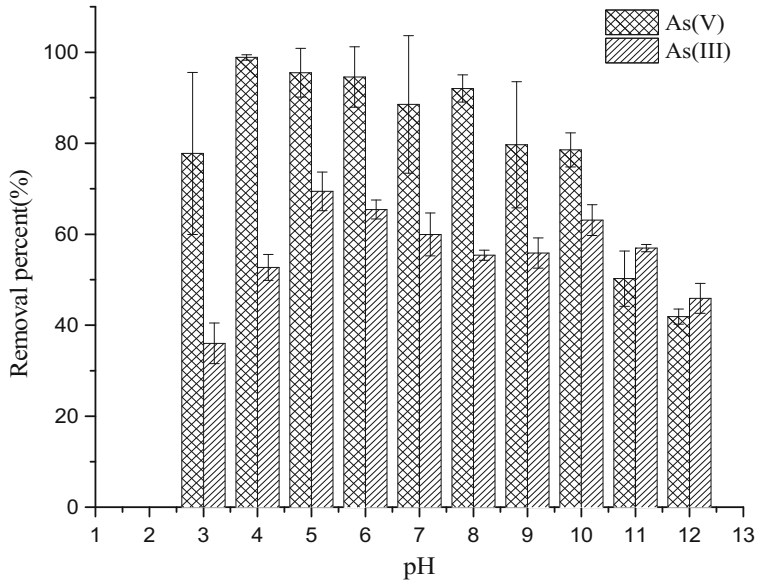

Fig. 5 Effect of pH on the adsorption of As(V) and As(III) by Fe-Y binary oxide. Arsenic initial concentration = 10 mg L^{-1}, adsorbent dose = 200 mg L^{-1}, and temperature = 25 °C

are illustrated in Fig. 6. The concentration of these coexisting anions was 100 mg L^{-1} (10 times of the arsenic concentration). It is noted from Fig. 6a that these anions of chloride, nitrate, and sulfate in aquatic solution displayed a weak impact on the removal of As(V). Only approximately 5 % of the initial As(V) (10 mg L^{-1}) remained in the solution after a 6-h reaction. However, the presence of phosphate strongly inhibited the uptake of As(V) by Fe-Y binary oxide. In the case, approximately 97 % of the initial As(V) still existed in the solution after the 6-h reaction, indicating that phosphate can strongly compete with arsenate for active adsorption sites on the surface of the adsorbent and significantly reduce the removal efficiency of As(V).

Compared with As(V), the adsorption of As(III) was obviously inhibited by chloride, nitrate, and sulfate and the residual percentage of As(III) after the 6-h reaction was still up to approximately 50 % of the initial As(III). The results imply that the affinity of As(III) to Fe-Y binary oxide is weaker than that of As(V). The existence of phosphate also exerted a strong suppression role in the adsorption of As(III).

It has been reported that chloride and nitrate could only form outer-sphere complex with ferric

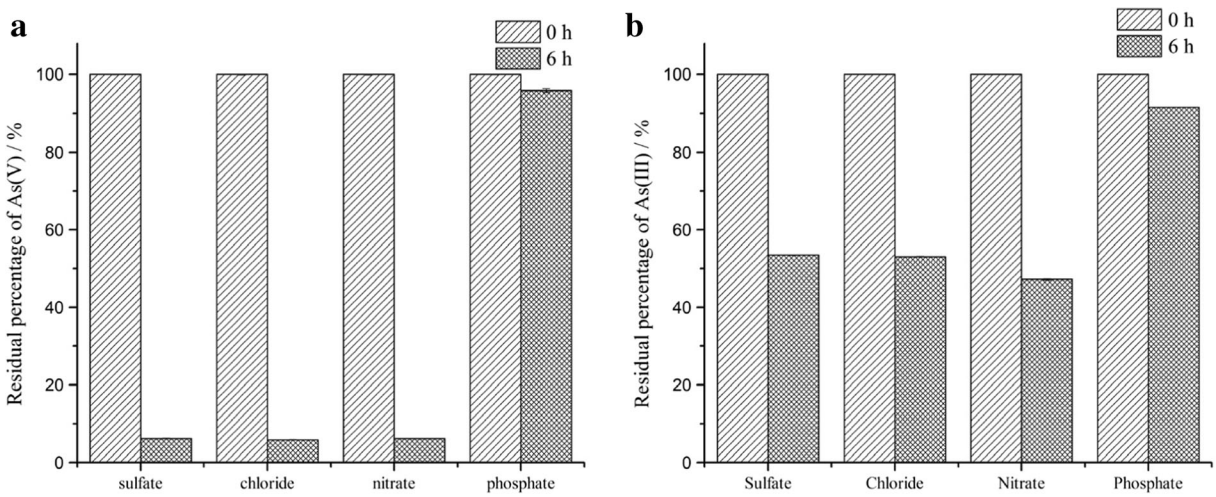

Fig. 6 Effect of co-existing anions on the adsorption of As(V) (**a**) and As(III) (**b**) by Fe-Y binary oxide. Arsenic initial concentrations = 10 mg L^{-1}, adsorbent dose = 200 mg L^{-1}, pH = 5.0, and temperature = 25 °C

hydroxides (Cumbal and Sengupta 2005). Sulfate would be also adsorbed predominantly via outer-sphere complexation at pH > 6 (Wijnja and Schulthess 2000; Lefèvre 2004). However, in this study, although the initial pH was 5, the solution pH will increase due to the release of OH^- ions (see Eqs. (2) and (3)). In the case, thus, sulfate may also form outer-sphere complex with Fe-Y binary oxide to compete with arsenic oxyanions, leading to a little reduction of arsenic removal rate like chloride and nitrate. It is known that arsenic and phosphorous are in the same group in the periodic table of elements. That means that these two elements' oxyanions have the similar physicochemical property. They both could form firmly bonded inner-sphere complex with Fe-Y binary oxide through the mechanism of ligand exchange. Therefore, the significant decrease in arsenic removal is observed in the presence of phosphate oxyanions.

3.6 XPS Analysis

To verify the presence of arsenic and examine its oxidation states on the adsorbent surface, XPS spectra of Fe-Y binary oxide before and after adsorbing As(V) and As(III) were analyzed and the results are illustrated in Fig. S1 and S2, respectively. As compared with the virgin adsorbent spectra (Fig. S1a), a new As 3d core level peak appeared in the spectra of Fe-Y binary oxide after the adsorbing As(V) and As(III) (Fig. S1b, c), clearly indicating the presence of arsenic on the surface of the adsorbent. And the binding energies for the adsorbent reacted with As(V) and As(III) are 45.23 and 44.28 eV (Fig. S2), which are very close to the reported values of 45.2~45.6 and 44.43~44.5 eV, respectively (Ouvrard et al. 2005; Zhang, et al. 2013). This means that the arsenic after adsorbed onto the adsorbent has no change in oxidation states, which is in agreement with the result reported by Ren et al. (2011).

4 Conclusions

In this study, Fe-Y binary oxide was synthesized and characterized to develop a novel and efficient adsorbent for the removal of arsenic from aqueous solution. The kinetic study indicates that the adsorption of As(III) and As(V) by the adsorbent can be well described by the pseudo-second-order kinetic model. The investigation on pH impact reveals that the adsorption of As(V) and As(III) is pH-dependent. The optimal pH for the adsorption of As(V) and As(III) is 4 and 5, respectively. The maximum capacity of As(V) and As(III) obtained in this study was 200 and 73 mg g^{-1}, respectively. The coexisting anions such as sulfate, chloride, and nitrate exerted a weak impact on the adsorption of As(V), but obviously inhibited the uptake of As(III). However, the presence of phosphate greatly suppressed the removal of both As(V) and As(III). In addition, it has been proven that Fe-Y binary oxide is magnetic, which is conducive to improve the efficiency of separation between adsorbent and wastewater.

Acknowledgments This study was supported by the National Natural Science Foundation of China (Grant No. 21377056).

References

Asadullah, M., Jahan, I., Ahmed, M. B., Adawiyah, P., Malek, N. H., & Rahman, M. S. (2014). Preparation of microporous activated carbon and its modification for arsenic removal from water. *Journal of Industrial and Engineering Chemistry, 20*, 887–896.

Bai, Y., Yang, T., Liang, J., & Qu, J. (2016). The role of biogenic Fe-Mn oxides formed in situ for arsenic oxidation and adsorption in aquatic ecosystems. *Water Research, 98*, 119–127.

Bellack, E. (1971). Arsenic removal from potable water. *Journal American Water Works Association, 63*, 454–458.

Bordoloi, S., Nath, S. K., Gogoi, S., & Dutta, R. K. (2013). Arsenic and iron removal from groundwater by oxidation-coagulation at optimized pH: laboratory and field studies. *Journal of Hazardous Materials, 260*, 618–626.

Cumbal, L., & Sengupta, A. K. (2005). Arsenic removal using polymer supported hydrated iron(III) oxide nanoparticles: role of donnan membrane effect. *Environmental Science & Technology, 39*, 6508–6515.

Jiang, B., Hu, P., Zheng, X., Zheng, J. T., Tan, M. H., Wu, M. B., & Xue, Q. Z. (2015). Rapid oxidation and immobilization of arsenic by contact glow discharge plasma in acidic solution. *Chemosphere, 125*, 220–226.

Karim, M. M. (2000). Arsenic in groundwater and health problems in Bangladesh. *Water Research, 34*, 304–310.

Kyzas, G. Z., Siafaka, P. I., Kostoglou, M., & Bikiaris, D. N. (2016). Adsorption of As(III) and As(V) onto colloidal microparticles of commercial cross-linked polyallylamine (Sevelamer) from single and binary ion solutions. *Journal of Colloid and Interface Science, 474*, 137–145.

Lee, J. Y., & Rosehart, R. G. (1972). Arsenic removal by sorption process from wastewaters. *Canadian Mining and Metallurgical Bulletin, 65*, 33–37.

Lefèvre, G. (2004). In situ fourier-transform infrared spectroscopy studies of inorganic ions adsorption on metal oxides and hydroxides. *Advances in Colloid and Interface Science, 107*, 109–123.

Li, T., Zhu, Z., Wang, D., Yao, C., & Tang, H. (2006). Characterization of floc size, strength and structure under various coagulation mechanisms. *Powder Technology, 168*, 104–110.

Martinson, C. A., & Reddy, K. J. (2009). Adsorption of arsenic(III) and arsenic(V) by cupric oxide nanoparticles. *Journal of Colloid and Interface Science, 336*, 406–411.

Mondal, P., Bhowmick, S., Chatterjee, D., Figoli, A., & Bruggen, B. V. (2013). Remediation of inorganic arsenic in groundwater for safe water supply: a critical assessment of technological solutions. *Chemosphere, 92*, 157–170.

Mondal, P., Hermans, N., Tran, A. T. K., Zhang, Y., Fang, Y. Y., Wang, X. L., & Bruggen, B. V. (2014). Effect of physicochemical parameters on inorganic arsenic removal from aqueous solution using a forward osmosis membrane. *Journal of Environmental Chemical Engineering, 2*, 1309–1316.

Ouvrard, S., Donato, P., Simonnot, M. O., Begin, S., Ghanbaja, J., Alnot, M., Duval, Y. B., Lhote, F., Barres, O., & Sardin, M. (2005). Natural manganese oxide: combined analytical approach for solid characterization and arsenic retention. *Geochimica et Cosmochimica Acta, 69*, 2715–2724.

Reddy, K. J., McDonald, K. J., & King, H. (2013). A novel arsenic removal process for water using cupric oxide nanoparticles. *Journal of Colloid and Interface Science, 397*, 96–102.

Ren, Z., Zhang, G., & Chen, J. P. (2011). Adsorptive removal of arsenic from water by an iron−zirconium binary oxide adsorbent. *Journal of Colloid and Interface Science, 358*, 230–237.

Ungureanu, G., Santos, S., Boaventura, R., & Botelho, C. (2015). Arsenic and antimony in water and wastewater: overview of removal techniques with special reference to latest advances in adsorption. *Journal of Environmental Management, 151*, 326–342.

Vrijenhoek, E. M., & Waypa, J. J. (2000). Arsenic removal from drinking water by a "loose" nanofiltration membrane. *Desalination, 130*, 265–277.

Wang, H. J., Gong, W. X., Liu, R. P., Liu, H. J., & Qu, J. H. (2011). Treatment of high arsenic content wastewater by a combined physical − chemical process. *Colloid and Surface A, 379*, 116–120.

Wasay, S. A., Haron, M. J., Uchiumi, A., & Tokunaga, S. (1996). Removal of arsenite and arsenate ions from aqueous solution by basic yttrium carbonate. *Water Research, 30*, 1143–1148.

Wijnja, H., & Schulthess, C. P. (2000). Vibrational spectroscopy study of selenate and sulfate adsorption mechanisms on Fe and Al (hydr)oxide surfaces. *Journal of Colloid and Interface Science, 229*, 286–297.

Yu, Y., & Chen, J. P. (2014). Fabrication and performance of a Mn-La metal composite for remarkable decontamination of fluoride. *Journal of Materials Chemistry, 2*, 8086–8093.

Yu, Y., Yu, L., & Chen, J. P. (2015). Introduction of an yttrium-manganese binary composite that has extremely high adsorption capacity for arsenate uptake in different water conditions. *Industrial and Engineering Chemistry Research, 54*, 3000–3008.

Zaitsev, V. S., Filimonov, D. S., Presnyakov, I. A., Gambino, R. J., & Chu, B. (1999). Physical and chemical properties of magnetite and magnetite-polymer nanoparticles and their colloidal dispersions. *Journal of Colloid and Interface Science, 212*, 49–57.

Zhang, Y., Yang, M., Dou, X. M., He, H., & Wang, D. S. (2005). Arsenate adsorption on an Fe–Ce bimetal oxide adsorbent: role of surface properties. *Environmental Science & Technology, 39*, 7246–7253.

Zhang, G. S., Qu, J. H., Liu, H. J., Liu, R. P., & Li, G. T. (2007). Removal mechanism of As(III) by a novel Fe–Mn binary oxide adsorbent: oxidation and sorption. *Environmental Science & Technology, 41*, 4613–4619.

Zhang, G. S., Khorshed, A. J., & Chen, J. P. (2012). Simultaneous removal of arsenate and arsenite by a nanostructured zirconium-manganese binary hydrous oxide: behavior and mechanism. *Journal of Colloid and Interface Science, 397*, 137–143.

Zhang, G., Ren, Z., Zhang, X., & Chen, J. (2013). Nanostructured iron(III)-copper(II) binary oxide: a novel adsorbent for enhanced arsenic removal from aqueous solutions. *Water Research, 47*, 4022–4031.

Zhang, L., Zhu, T., Liu, X., & Zhang, W. (2016). Simultaneous oxidation and adsorption of As(III) from water by cerium modified chitosan ultrafine nanobiosorbent. *Journal of Hazardous Materials, 308*, 1–10.

Zhao, D., Yu, Y., & Chen, J. P. (2016). Zirconium/polyvinyl alcohol modified flat-sheet polyvinyldene fluoride membrane for decontamination of arsenic: material design and optimization, study of mechanisms, and application prospects. *Chemosphere, 155*, 630–639.